



Three-dimensional tomographic reconstruction and MHD modeling of the low Corona during the last three solar minima

Diego Lloveras¹, A. Vásquez², F. Nuevo², R. Frazin³, W. Manchester IV³, C. Mac Cormack⁴, N. Sachdeva³, B. Van der Holst³ and P. Lamy⁵

¹Grupo de estudios Heliofísicos de Mendoza, U. de Mendoza, Arg. ([GEHME](#))

²Instituto de Astronomía y Física del Espacio (CONICET-UBA), Arg. ([IAFE](#))

³Department of Climate and Space Sciences and Engineering, U. of Michigan, USA. ([CLASP](#))

⁴Heliospheric Physics Laboratory, Heliophysics Science Division, NASA Goddard Space Flight Center, USA. ([NASA](#))

⁵Laboratoire Atmosphères, Milieux et Observations Spatiales, France. ([LATMOS](#))

Coronal radiation

Radiation from the corona is caused by different phenomena

- Corona-K: Thomson scattering of WL, observable with coronographs.
- Corona-E: Electronic decay of Iron ions emitting in EUV.

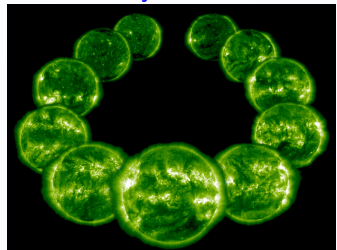
EUV images of a complete solar cycle. Images taken in the 195Å band of the EIT/SoHO instrument.

- The maximum phase shows a large number of ARs and these appear in two well-defined latitude bands.
- The minimum phase shows a marked decrease in ARs, characterizing the quiescent corona.

Minimum in white light



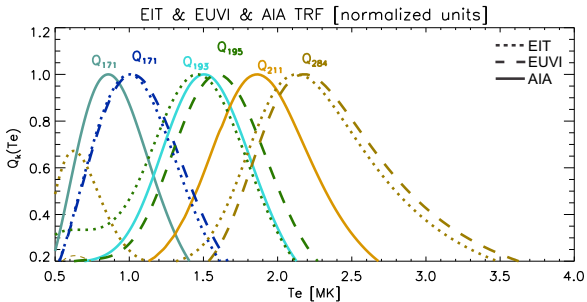
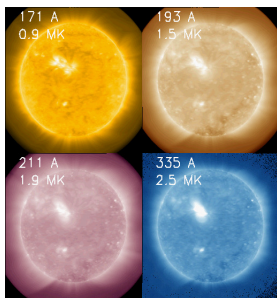
Solar cycle in EUV



Temperaturas características de la corona solar

Los telescopios espaciales tienen detectores EUV, cuyos filtros seleccionan principalmente líneas de Fe ($T_e \sim 0.5 - 2.5$ MK).

$$Q_k(T) \equiv \int d\lambda \phi_k(\lambda) \eta(N_{e0}, a_0, T; \lambda) / N_{e0}^2$$



- ϕ_k : Pasabandas k
- $\eta(\lambda, T)$: Modelo de Emisividad CHIANTI.

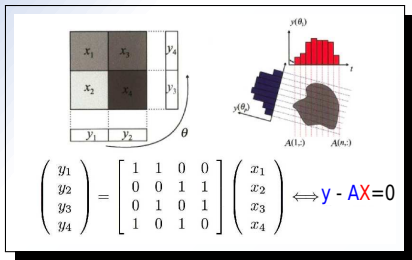
Lloveras et al. (2018)

Tomography

Unknown: 3D distribution of a certain quantity x_i (e.g. N_e) for each cell volume i within an object (e.g. the solar corona), under optically thin regime (e.g. WL)

Knowns:

- **Intensity vector y_j :** measurement in each **pixel j** of each image of a time-series providing different view angles.
- **Projection matrix A_{ji} :** depending on the **geometry** (e.g. solar rotation, telescope orbit) and the involved **physical process** (e.g. Thomson scattering).



Tomographic reconstruction
C2-SRT (N_e) $2.5 - 6.5 R_\odot$
EUV-SRT (N_e, T_e) $1.0 - 1.3 R_\odot$

- **Solar Rotational Tomography:** it is the solar rotation itself that provides the different viewing angles.

The SRT Problem

The signal recorded by the j -th pixel is given by:

$$I_j = \int_{\text{LOS}_j} dl w(l) x(l) \rightarrow I = A \cdot X$$

I : Vector of J elements I_j , all pixels in all images.

A : Large sparse matrix of $J \times I$ elements $a_{j,i}$, purely geometrical.

X : Vector of I elements x_i , the discrete 3D distribution of the unknown:

WL-SRT

$$x(r) = N_e(r)$$

$$w(r) = S_{\text{Thomson}}(r)$$

EUV-SRT

$$x(r) = FBE_k(r) \equiv \int_0^{\infty} d\lambda \phi_k(\lambda) \eta(r, \lambda)$$

$$w(r) = 1$$

Solution: global optimization problem with cost function (of dimension- I):

$$f(X) = \|I - A \cdot X\|^2 + p \|R \cdot X\|^2$$

1st term: Difference between data and synthetic images.

2nd term: Regularization of the solution.

Imágenes Dato

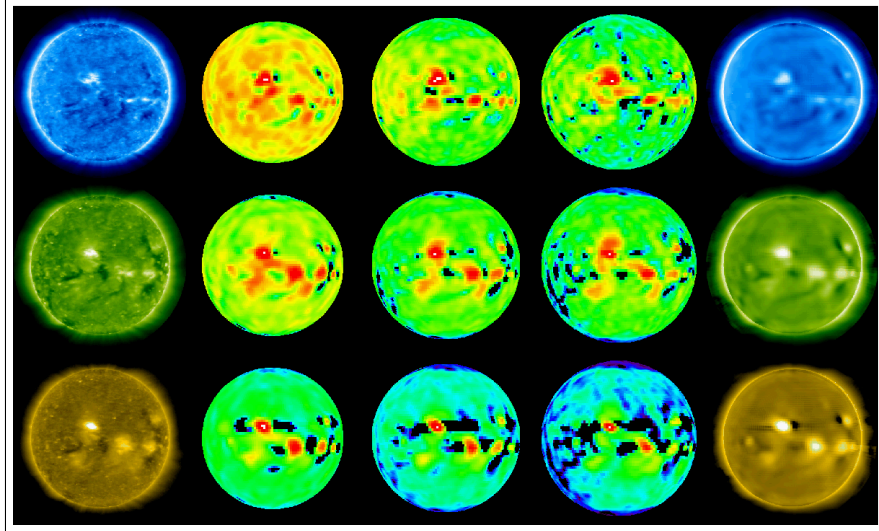
→

3D FBE

→

Imágenes Sintéticas

171 Å



$1.035 R_{\odot}$

$1.085 R_{\odot}$

$1.135 R_{\odot}$

Vásquez et al. (2009)

Local Differential Emission Measure (LDEM)

- En cada celda tomográfica i se conocen K FBEs.
- Utilizando las Respuestas Térmicas $Q_k(T)$
- Las FBEs pueden reescribirse como: $FBE_{k,i} = \int dT Q_k(T) LDEM_i(T)$.
- Donde la $LDEM_i(T)$ [$\text{cm}^{-6}\text{K}^{-1}$] para cada celda i se define tal que:

$$N_{m,i}^2 = \langle N_e^2 \rangle_i = \int dT LDEM_i(T)$$

$$T_{m,i} = \langle T_e \rangle_i = \frac{1}{\langle N_e^2 \rangle_i} \int dT T LDEM_i(T)$$

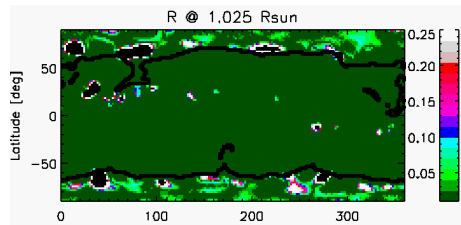
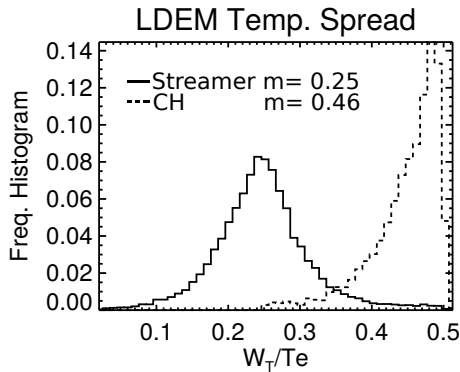
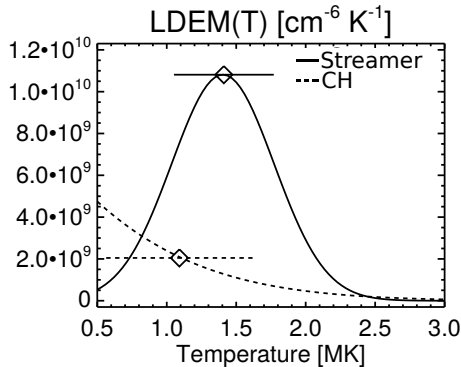
$$W_{T,i}^2 = \frac{1}{\langle N_e^2 \rangle_i} \int_{T_{min}}^{T_{max}} dT LDEM_i(T) (T - \langle T_e \rangle_i)^2$$

- Se modela la LDEM: $LDEM_i(T) = \mathcal{N}(T, \lambda_i = [A, T_0, \sigma_T])$ Nuevo et al. (2015)
- La siguiente función objetivo es minimizada en cada celda:

$$\Phi(\lambda_i) = \sum_k |FBE_{k,i} - \int dT Q_k(T) \mathcal{N}(T, \lambda_i)|^2.$$

- Grado de éxito $R_i \equiv (1/K) \sum_k |1 - FBE_{k,i} / \int dT Q_k(T) \mathcal{N}(T, \lambda_i)|$

Typical LDEM

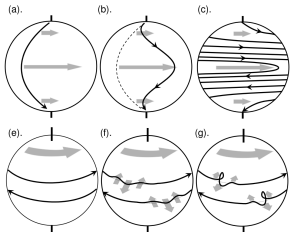


Lloveras et al. (2022)

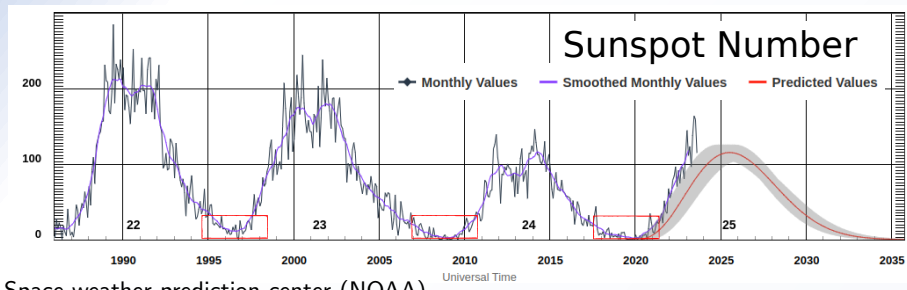
$$R \sim 1\% \text{ (Streamer)} \quad y \sim 10\% \text{ (CHs)}$$

The Solar cycle and the Coronal Activity

Babcock et al. (1961)



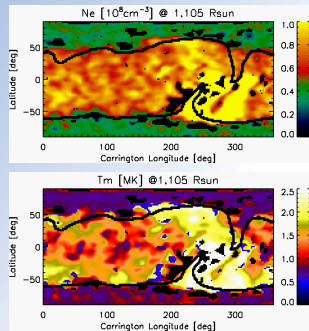
- Solar dynamo $\rightarrow B(t)$.
- Mínima: Global dipolo, few SSs/ARs.
- Maxima: Multipole, many SSs/ARs.
- Period ~ 11 years



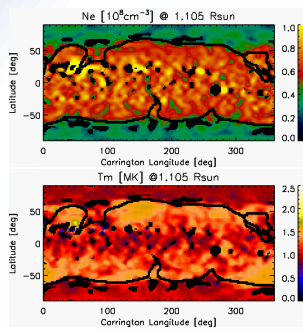
Space weather prediction center (NOAA)

EUV-SRT Comparative Solar Minima Study

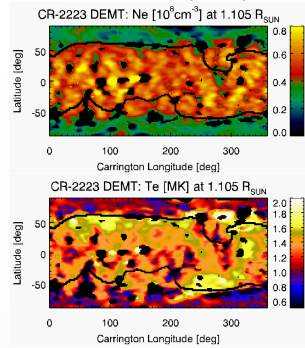
CR-1915 (EIT)



CR-2081 (EUVI)



CR-2223 (AIA)

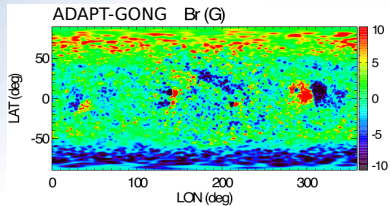
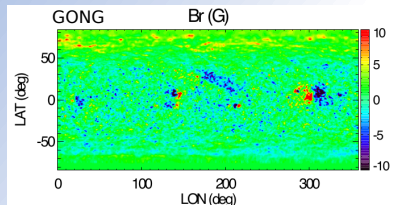


Lloveras et al. (2017,2020,2022)

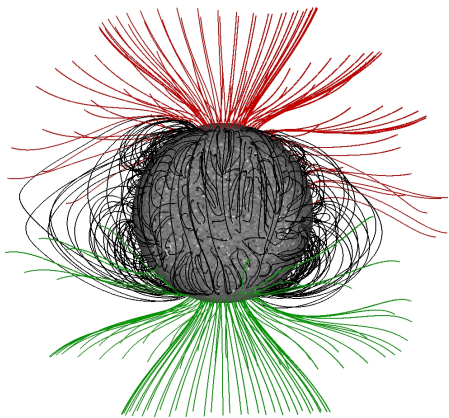
- Azimuth symmetry
- Streamer(CHs) → higher(lower) density and temperature.
- Maximum gradients at O/C boundary

3D magnetic model

Sinoptic magnetogram (~ 28 days)

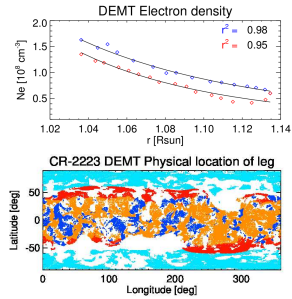
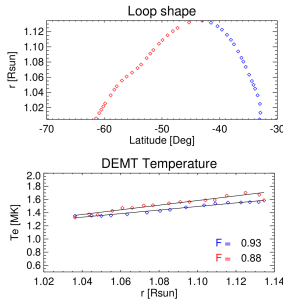
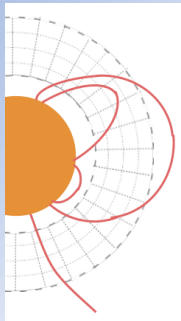


PFSS



- Assimilation Photospheric Flux Transport (ADAPT, Worden and Harvey, 2000): applies a magnetic flux transport model.

Tomographic Results along B-lines



Results along individual B-lines are characterized by parametric fits:

$$N_e^{(\text{EUV-SRT})} = N_0 \exp[-(h/\lambda_N)]$$

$$T_m = ar + b$$

and fitting parameters are analyzed statistically

UP ($a \equiv dT_e/dr > 0$)

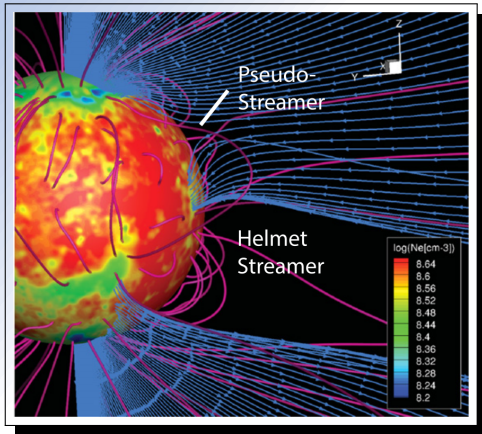
DOWN ($a \equiv dT_e/dr < 0$)

Type	Characteristic
0	Closed Small Down
I	Closed Small Up
II	Closed Large Up
III	Open Large Up

EUV-SRT conclusions during deep minima

- ▷ General characteristics:
 - Streamers exhibit $N_{CB} \approx 1.0 - 1.2 \times 10^8 \text{ cm}^{-3}$, CHs are characterized by half of that density.
 - $\lambda_N \approx 7 - 11 \times 10^{-2} R_\odot$, the lower values corresponding to the lower latitudes of the streamer and CHs.
 - Streamers are characterized by $\langle T_m \rangle \approx 1.2 - 1.6 \text{ MK}$ (the lowest temperatures corresponding to lower latitudes) while CHs exhibit $\langle T_m \rangle \lesssim 1 \text{ MK}$.
 - Loops with $dT_e/dr < 0$ systematically found in the Streamer core of all minima → reproduced by Alfvén wave heating models (Schiff & Cranmer, 2016) → Presents conditioning to the coronal heating model.
- ▷ Comparison of the last 3 minima:
 - $\langle T_m^{SC\ 22/23} \rangle > \langle T_m^{SC\ 23/24} \rangle \lesssim \langle T_m^{SC\ 24/25} \rangle$
 - $N_{CB}^{SC\ 22/23} > N_{CB}^{SC\ 23/24} > N_{CB}^{SC\ 24/25}$
 - The global thermodynamic state of minima is not correlated with the activity level of a full cycle.

Space Weather Modeling Framework



- Developed at CLaSP / U. of Michigan
(Toth et al. 2012)
- Model Sun – Heliosphere – IM
- Multiple modules
- AWSoM: SC and IH
Coronal heating given by dissipation of Alfvén waves (van der Holst et al., 2014).
- Synoptic Magnetogram as Boundary Condition (ADAPT-GONG)

Jin et al. 2012; Evans et al. 2012
Oran et al. 2015; Sachdeva et al. 2019
Lloveras et al. 2020,2022

Modelo MHD de la corona global (AWSoM)

- Cond. de contorno ADAPT-GONG → PFSS
- Región de Transición extendida
- Conserv. masa, inducción, divergencia nula
- Conserv. del momento:

$$\frac{\partial}{\partial t}(\rho \vec{v}) + \nabla \cdot \left[\rho \vec{v} \vec{v} + (p_i + p_e + \textcolor{blue}{p}_A + \frac{1}{2\mu_0} B^2) \vec{I} - \frac{\vec{B}\vec{B}}{\mu_0} \right] = -\rho \frac{GM_\odot}{r^3} \vec{r}$$

- Ecuaciones de energía:

$$\frac{\partial}{\partial t} \left(\frac{1}{2} \rho v^2 + \frac{p_i}{\gamma-1} + \frac{1}{2} B^2 \right) + \nabla \cdot \left[\left(\frac{1}{2} \rho v^2 + \frac{\gamma p_i}{\gamma-1} + B^2 \right) \vec{v} - \vec{v} \cdot \vec{B} \vec{B} \right] = \frac{N_i k_b}{\tau_{ei}} (T_e - T_i) + \textcolor{red}{Q}_i$$

$$\frac{\partial}{\partial t} \left(\frac{p_e}{\gamma-1} \right) + \nabla \cdot \left(\frac{\gamma p_e}{\gamma-1} \vec{v} \right) + \nabla \cdot \left(\textcolor{blue}{p}_A \vec{v} \right) = -\nabla \cdot \vec{q}_e + \frac{N_i k_b}{\tau_{ei}} (T_i - T_e) - Q_{rad} + \textcolor{red}{Q}_e$$

- Densidad de energía de ondas de Alfvén:

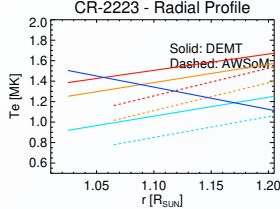
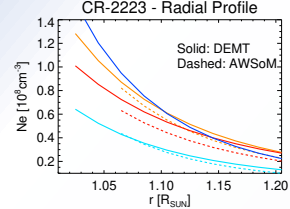
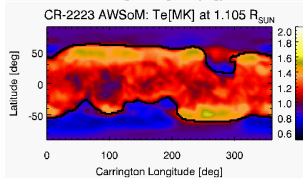
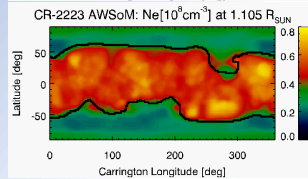
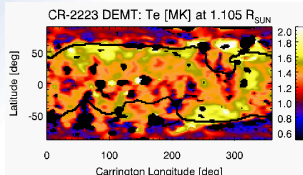
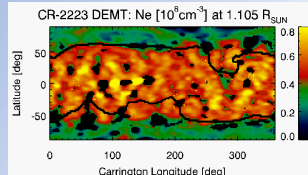
$$\frac{\partial w_\pm}{\partial t} + \nabla \cdot [(v \pm V_A) w_\pm] = -\frac{w_\pm}{2} (\nabla \cdot v) - \Gamma_\pm w_\pm \mp R \sqrt{w_- w_+}$$

$$\Gamma_\pm = \frac{2}{L} \sqrt{\frac{w_\mp}{\rho}} \quad \text{Dmitruk et. al (2002)} \quad \textcolor{red}{Q}_i + \textcolor{red}{Q}_e = \Gamma_+ w_+ + \Gamma_- w_- \quad \textcolor{blue}{p}_A = (w_+ + w_-)/2$$

van der Holst et al. (2014)

Sachdeva et al. (2019,2021); Lloveras et al. (2022)

EUV-SRT validation of AWSoM



- Good agreement in magnitude and morphology of structures.

- Good agreement North O/C boundary and CH

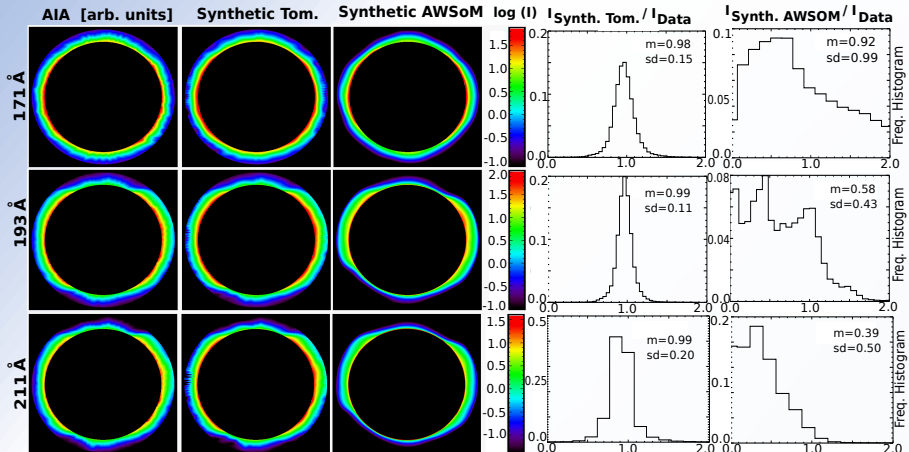
- Southern O/C boundary shifted $+20^\circ$ from CH

- $\Delta T_e(r) \sim -15\%$

- $\Delta N_e(r) \sim 5\%$

(Lloveras et al. 2022)

EUV Synthetic Images: EUV-SRT vs AWSOM

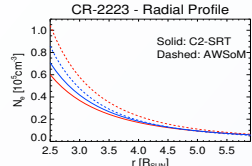
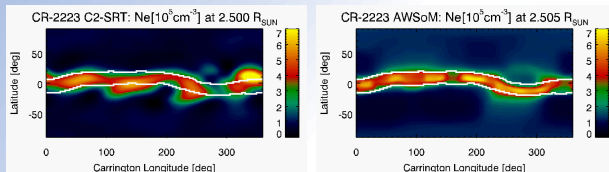


$$I_{Synt} \sim \int_{LoS} dI N_e^2 Q_k$$

- AWSOM O/C discrepancy due to lack of accuracy of boundary condition.

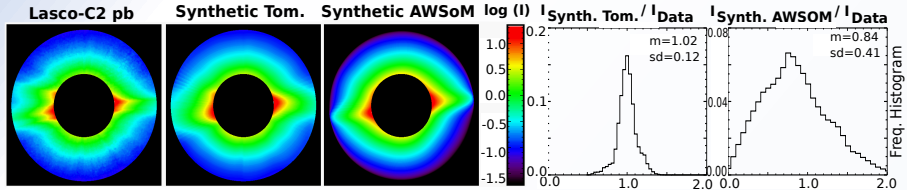
(Lloveras et al. 2022)

WL-SRT Validation of AWSoM



- Good overall consistency in shape and size of streamer y CHs.

$$N_e^{(C2-SRT)}(r) = N_0 \left(r/2.5 R_\odot \right)^{-p} \rightarrow \langle \lambda_N \rangle = \frac{\langle r \rangle}{p}$$



- $N_e(r = 2.5 R_\odot) \approx 0.6 - 0.7 \times 10^5 \text{ cm}^{-3}$
- $\lambda_N \approx 1.4 - 1.6 R_\odot \rightarrow \langle p \rangle \approx 2.8 - 3.3$ (consistent with other studies)
- AWSoM overestimates basal density by up to +75% → model's acceleration rates are too low.
(Lloveras et al. 2022)

$$I_{Synt} \sim \int_{LoS} dI / N_e$$

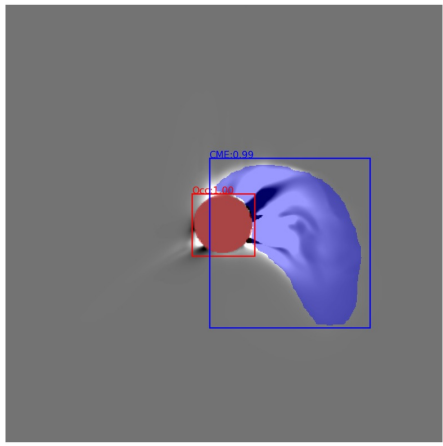
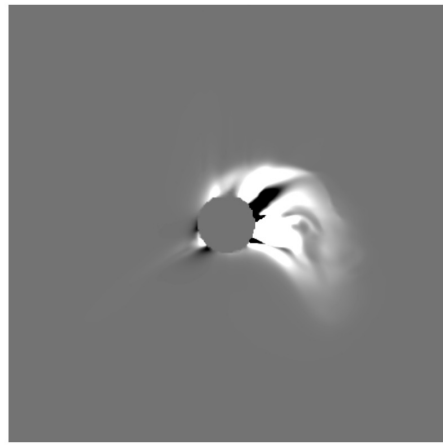
Observational validation of CME simulation

- 1 - Validation of background Corona (Umich+IAFE+Gehme)
 - SRT to validate AWSoM
- 2 - CME segmentation (Gehme)
 - Select runs that are similar to data.
- 3 - Diagnostic Tools (Gehme)
 - Compare intensity profiles between data and synthetic images.

2 - CME segmentation

- Deep Neural Networks trained to identify and segment the outer envelope of CMEs in single differential coronagraph images, producing a GCS-like mask.

Synthetic Images (cor2B, event 2011-15-02, run 005)



3 - Diagnostic imaging

- Event/pre-event ratio images from STEREO-B/COR2 point of view.

